# Investigations of the Solar Corona by VLBI

Benedikt Soja, Robert Heinkelmann, Harald Schuh

**Abstract** The solar corona is an important target for solar research and the understanding and prediction of space weather. Several techniques have been applied in the past to determine properties of the corona, most notably, its electron density. Recently, for the first time, it was shown by the authors that Very Long Baseline Interferometry (VLBI) is capable of assessing the characteristics of the solar corona. For this paper, further investigations were performed. The electron density models were compared to those from spacecraft tracking, and correlations between solar activity, characterized by Sunspot numbers, and the electron density have been studied. In addition, the temporal variations of the density and turbulence of the corona were investigated. Here, a comparison between VLBI and coronagraph data shows that VLBI is sensitive to transient events such as coronal mass ejections.

**Keywords** Solar corona, ionosphere, VLBI, electron density, Coronal Mass Ejection

## 1 Introduction

The solar corona is a dispersive medium for electromagnetic waves. By conducting radio measurements to targets with small angular distances to the Sun, it is possible to determine the electron density of the coronal plasma. In the past 45 years, models of the electron density have been derived by various techniques [1], most notably spacecraft tracking during superior solar conjunctions [2].

Recently, geodetic VLBI data has been used to successfully determine electron density models of the corona [3, 4]. A slightly different approach, combining VLBI and GNSS data, has led to similar outcomes [5]. While VLBI is not as precise as spacecraft tracking in sensing the coronal electron content, it offers the possibility of probing the corona on a regular basis because it does not depend on superior solar conjunctions with spacecraft. Furthermore, VLBI is able to observe several radio sources at the same time, allowing the study of electron density variations in various regions around the Sun.

GFZ German Research Centre for Geosciences, Potsdam, Germany

## 2 Data and Methodology

The electron density models from VLBI data are based on twelve R&D experiments performed by the International VLBI Service for Geodesy and Astrometry (IVS) [6] in 2011 and 2012. Each of the sessions utilized a global network of up to nine radio telescopes, lasted 24 hours, and included observations with solar elongation angles less than 15°, which had been the cut-off elongation angle between 2002 and 2013. The derived group delays in S- and X-band allowed the computation of the dispersive contribution to X-band $\tau_{disp,x}$ which is the observable used in a least-squares adjustment to estimate instrumental dispersive delays, parameters of the Earth's ionosphere, and, of most interest, of the solar corona. The coronal electron density is parameterized using a radial power-law

$$N_e(r) = N_0 \cdot r^{-\beta} \tag{1}$$

with the electron density at the Sun's surface $N_0$, the fall-off parameter $\beta$, and the heliocentric distance $r$ in units of solar radii $R_\odot$. More details about the dataset and methodology can be found in [4].

## 3 Results and Discussion

### 3.1 Comparison with Electron Density Models from Spacecraft Tracking

We have compared the average electron density model derived from the twelve VLBI experiments with previous models obtained from radio measurements to spacecraft during superior solar conjunctions. In Table 1, models derived between 1970 and 2008 are included (spacecraft Mariner 6/7, Viking 1/2, Voyager 2, Ulysses, Mars Express, and Rosetta [2]), as well as the model from VLBI data. The spacecraft tracking data are distributed over a period of almost 40 years and were obtained during very different solar conditions. The different fall-off parameters $\beta$ range from about 2.1 to 2.5. The electron density at a distance of 14 $R_\odot$ varies by a factor of two (excluding the value for Voyager in 1988 – the electron density is about four to eight times larger compared to other models). The model from VLBI data agrees well with the spacecraft-based ones.

**Table 1** Power-law parameters $N_0$ and $\beta$ of the models derived from spacecraft tracking and VLBI data are given. Additionally, for each data set, the minimum elongation, smoothed Sunspot numbers during the data acquisition, and the electron density at a distance of 14 $R_\odot$ are included.

| Mission / data set | Year | Min. elongation | $N_0$ [$10^{12}$ m$^{-3}$] | $\beta$ | $N_e(14\,R_\odot)$ [$10^9$ m$^{-3}$] | SSN |
|---|---|---|---|---|---|---|
| MAN 6/7 | 1970 | 1.6° | 0.60 | 2.06 | 2.61 | 105 |
| VIK 1/2 | 1976 | 0.8° | 0.99 | 2.32 | 2.17 | 13 |
| VOY 2 | 1985 | 1.7° | 1.92 | 2.36 | 3.79 | 18 |
| VOY 2 | 1988 | 1.4° | 6.04 | 2.25 | 15.93 | 100 |
| ULS | 1991 | 1.4° | 2.85 | 2.47 | 4.21 | 145 |
| MEX | 2004 | 1.0° | 1.68 | 2.46 | 2.55 | 40 |
| ROS | 2006 | 2.2° | 0.84 | 2.14 | 2.96 | 15 |
| MEX | 2008 | 2.5° | 0.49 | 2.07 | 2.08 | 3 |
| VLBI | 2012 | 3.9° | 1.24 | 2.3 | 2.87 | 58 |

### 3.2 Dealing with the Parameter $\beta$

Using VLBI data, it has only been possible to determine one of the power-law parameters $N_0$ and $\beta$ due to correlations between them. In this section, we investigate, to which extent different fixed values of $\beta$ affect the estimated electron density models from VLBI.

Table 2 shows the estimated power-law parameter $N_0$ for several $\beta$ values 2.0, 2.3, and 2.6. Additionally, the corresponding electron densities at distances 14 and 20 $R_\odot$ are displayed. It is evident that $N_0$ and $\beta$ are correlated (correlation coefficient 0.97 for a sample of seven $\beta$ values between 2.0 and 2.6). Larger values of $\beta$ (i.e., a steeper decline) lead to higher theoretical electron densities at the surface of the Sun. At 3.9° elongation ($\approx 14\ R_\odot$) and farther away (i.e., the distances at which observations were performed), the difference in the electron density $N_e$ is significantly lower compared to $N_0$. When assuming $\beta = 2.3$ for our VLBI model, the difference to the other estimates shown in Table 2 is about $4 \cdot 10^7$ m$^{-3}$ at 14 $R_\odot$, about 4% of the standard error (68% confidence interval). Within the range, where the VLBI model is valid, the largest absolute difference is found at 20 $R_\odot$: about $1.5 \cdot 10^8$ m$^{-3}$ with a gradient $\Delta N_e/\Delta\beta$ of about $-5 \cdot 10^8$ m$^{-3}$. Here, the difference amounts to roughly $\frac{1}{3}\sigma$, which is still insignificant.

**Table 2** The table shows the average electron density models derived from all twelve R&D sessions fixing the value of $\beta$ to 2.0, 2.3, and 2.6. Included are the electron densities at 1 (theoretical value $N_0$), 14, and 20 $R_\odot$ (3.8° and 5.4° elongation) together with their standard errors.

| $\beta$ | $N_0$ [$10^{12}$ m$^{-3}$] | $N_e(14\,R_\odot)$ [$10^9$ m$^{-3}$] | $N_e(20\,R_\odot)$ [$10^9$ m$^{-3}$] |
|---|---|---|---|
| 2.0 | $0.57 \pm 0.18$ | $2.91 \pm 0.92$ | $1.42 \pm 0.45$ |
| 2.3 | $1.24 \pm 0.42$ | $2.87 \pm 0.97$ | $1.26 \pm 0.43$ |
| 2.6 | $2.70 \pm 0.98$ | $2.83 \pm 1.03$ | $1.12 \pm 0.41$ |

Figure 1 shows the VLBI model for three different values of $\beta$ (see Table 2) compared to previous models developed from spacecraft tracking (Table 1). The differences between the three VLBI models are small at the elongations at which VLBI observations have been performed. At closer elongations, e.g. 2°, the differences are larger, but the electron densities are still within the range suggested by previous models. The deviation of the 1988 Voyager 2 model (uppermost line

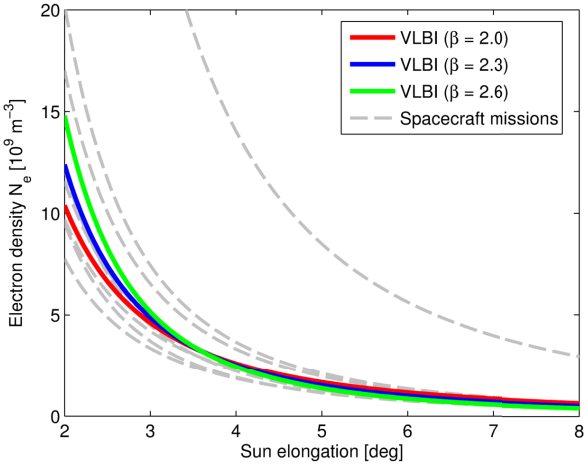


**Fig. 1** The electron density models from VLBI data using three different values of $\beta$ (see Table 2) are compared to models from spacecraft tracking. The electron densities of the coronal plasma are plotted as functions of solar elongation.

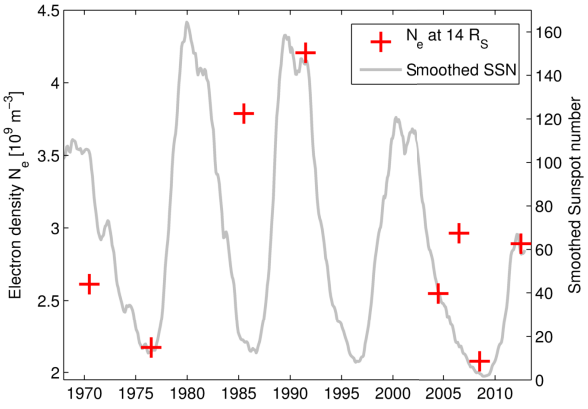


**Fig. 2** The electron densities at a heliocentric distance of 14 $R_\odot$ from the models in Table 1 are plotted together with a time series of smoothed Sunspot numbers (SSN). The model from the 1988 Voyager 2 conjunction was excluded.

in Figure 1, separated from all other models) is much larger than those caused by different $\beta$ values.

Bird et al. [2] have suggested that a correlation between $\beta$ and solar activity exists. Since our data is from a period of medium solar activity, a medium value of $\beta = 2.3$ is appropriate.

### 3.3 Comparison to Sunspot Numbers

In Figure 2 we investigate whether correlations between the models from Table 1 and smoothed Sunspot numbers, which are indicators for overall solar activity, can be found. The electron densities in this figure are assessed at a distance of 14 $R_\odot$ (cf. Table 1). The reason for not using $N_0$ in this comparison is the strong correlation between $N_0$ and $\beta$ as explained in Section 3.2.

Besides the model from 1988 (which was not considered in Figure 2), the ones from 1985 and 2006 (spacecraft Voyager 2 and Rosetta, respectively) also show, to a minor extent, anomalous electron densities when compared to smoothed SSN. The correlation between $N_e(14\,R_\odot)$ and SSN is 41% for all models, 55% when excluding the one from 1988, and 88% when further excluding the ones from 1985 and 2006.

For the outlying model from 1988 and also for the slightly anomalous models from 1985 and 2006, observations in regions of higher electron density are responsible [7, 8]. The average VLBI model is not affected to the same extent by such regional anomalies because the spatio-temporal sampling of the observations is more broadly distributed when compared to spacecraft tracking.

### 3.4 Coronal Mass Ejection Identifications through Coronagraph and VLBI Data

Coronal mass ejection (CME) events cause a regional and time-limited increase in electron density and turbulence. Increases in coronal total electron content (TEC) observed by spacecraft could be linked to such events in the past [7]. Thus, it is of interest studying the VLBI observations for similar TEC time variations. The problem is, a single VLBI observation is only sensitive to the difference in TEC along the lines-of-sight of the two telescopes, which strongly depends on the orientation and length of the baseline. If the electron density was strictly radially symmetric, this dependency could be removed by scaling with the inverse of the projected baseline $b_\perp \doteq p_2 - p_1$ with the impact parameters $p_i$ of the two ray paths. However, the scatter due to turbulance and small-scale variations in electron density is unnaturally amplified for small $b_\perp$ which makes the detection of time variations in TEC impossible.

Instead, the increase in turbulence caused by the CMEs was investigated using the formal errors of the dispersive group delays. The formal errors (in terms of $1\sigma$ standard deviations) are determined during the correlation of the VLBI signals and are indirectly proportional to the geometric mean of antenna temperatures [9, 10]

$$\sigma_\tau \propto \frac{1}{\sqrt{T_{A_1} \cdot T_{A_2}}} \ , \tag{2}$$

which are in turn proportional to the effective flux density of the observed source. Thus, if the flux density is reduced due to perturbations, e.g., in the corona, the formal errors $\sigma_\tau$ are expected to increase. The formal errors of the dispersive contribution in X-band can be derived from $\sigma_\tau$ in S- and X-band by

$$\sigma_{\tau_{disp,x}} = \sqrt{\sigma_{\tau_x}^2 + \sigma_{\tau_s}^2} \cdot \frac{f_s^2}{f_x^2 - f_s^2} \ . \tag{3}$$

During the twelve R&D sessions, two CMEs took place in coronal regions through which radio sources were observed. Figure 3 shows time series of the formal errors $\sigma_{\tau_{disp,x}}$ for the observations of radio source 2008-159 (RD1201) and 1243-072 (RD1208) during CME events. The radio source 1958-179 was even closer to the path of the CME during RD1201, but was only observed during the first half of the session, i.e., before the CME happened. Also included in this figure are LASCO [11] coronagraph images depicting the evolution of the CMEs and the positions of the observed radio sources (more details about these images, as well as animations can be found in [4]). Since the observations in Figure 3 are from different baselines with telescopes of different sizes and receiver hardware, the standard deviations are scattered. Still, a trend is visible. At about the same time when the brighter plasmas arrive at the ray paths of the telescopes pointing to the respective radio sources (about 12 PM for RD1201 and 9 AM for RD1208), a strong increase in the formal errors appears.

In both cases the standard deviations increase even a bit earlier. Consequently, there seems to be an increase in turbulence before the bright plasma of the CME arrives at the line-of-sight as seen in the LASCO images. Another reason could be disturbances in the Earth's ionosphere, but time series of ionospheric TEC do not show any anomalies in this specific time period.

Also indicated in Figure 3 are the quality codes from the correlation. Diamonds represent observations of low quality which are not used in standard VLBI analysis (and also not in this study for estimating the coronal electron density). At roughly the same time when the CMEs pass the ray paths, most observations are flagged as low quality.

## 4 Conclusions

We have shown that the model from VLBI data fits well to ones from spacecraft tracking. A correlation close to 90% between selected electron density models of the past (including the one from VLBI) and Sunspot numbers exists. While we cannot give an independent estimate of the power-law parameter $\beta$, we have demonstrated that the arbitrary choice does not affect the resulting electron density models significantly. Finally, the effects of coronal mass ejections, identified through coronagraph images, have also been detected in the VLBI data.

## Acknowledgements

The authors thank the IVS for observing, correlating, and providing the VLBI data used in this work. The LASCO data used here are produced by a consortium of the Naval Research Laboratory (USA), Max-Planck-Institut für Radioastronomie (Germany), Laboratoire d'Astronomie (France), and the University of Birmingham (UK).

## References

1. P. B. Esposito, P. Edenhofer, and E. Lueneburg. Solar corona electron density distribution. *J. Geophys. Res.*, 85:3414–3418, 1980.
2. M. K. Bird, M. Pätzold, B. Häusler, S. W. Asmar, S. Tellmann, M. Hahn, A. I. Efimov, and I. V. Chashei. Coronal radio sounding experiments with the ESA spacecraft MEX, VEX, and Rosetta. In *511th WE-Heraeus-Seminar, Bad Honnef, Germany, Jan 31 - Feb 3 2012*. 2012.
3. B. Soja, J. Sun, R. Heinkelmann, H. Schuh, and J. Böhm. Sun Corona Electron Densities Derived from VLBI Sessions in 2011/2012. In *Proceedings of the 21st Meeting of the European VLBI Group for Geodesy and Astrometry*, N. Zubko and M. Poutanen, editors, pages 159–163, 2013.

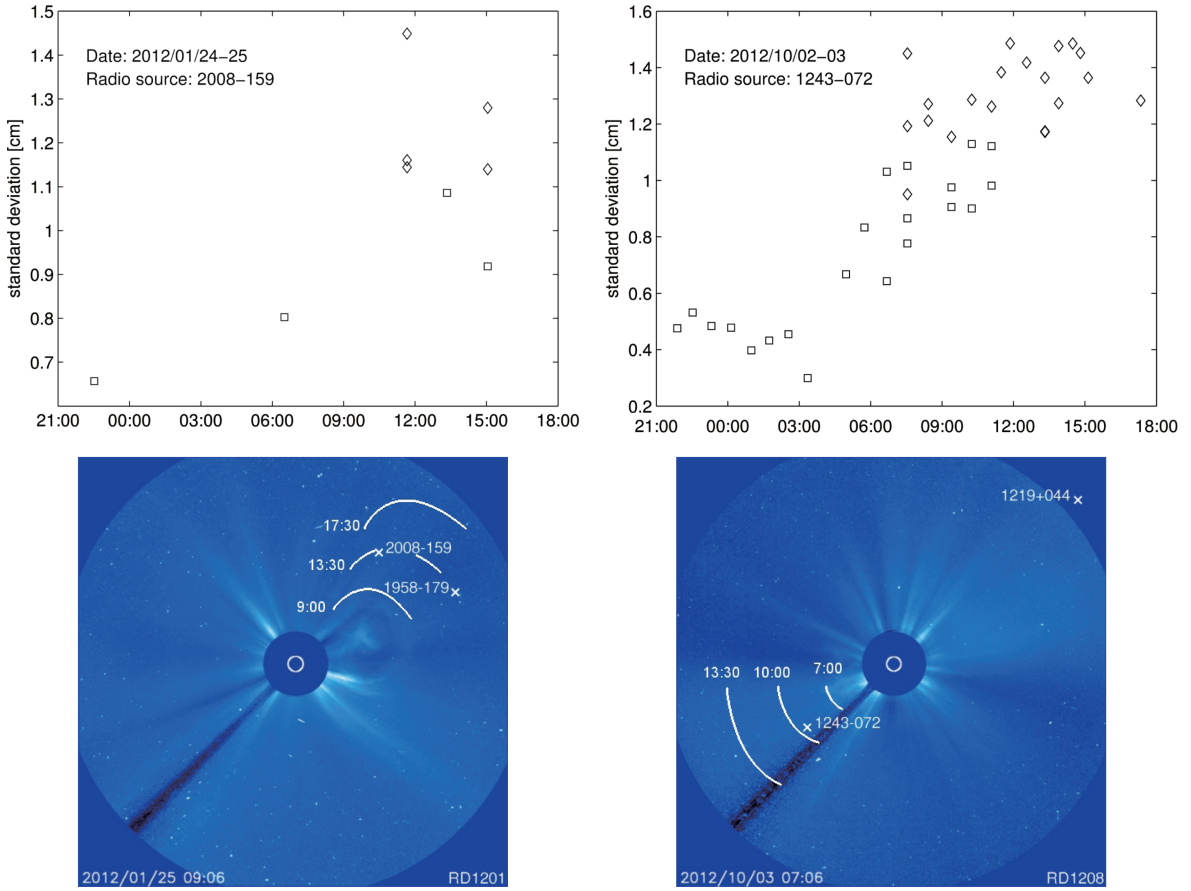


**Fig. 3** The a priori standard deviations of the dispersive delay observations, as estimated in the correlation of the VLBI data, for sessions RD1201 on 2012/01/24–25 (top left) and RD1208 on 2012/10/02–03 (top right). Squares indicate decent quality observations, and diamonds stand for observations with bad correlation quality flags. The bottom figures show the positions of the radio sources (white crosses) in the vicinity of the Sun with respect to images of the LASCO C3 coronagraph. The temporal evolution of the CMEs is indicated by white curves.


4. B. Soja, R. Heinkelmann, and H. Schuh. Probing the Solar Corona with Very Long Baseline Interferometry. *Nature Communications*, submitted, 2014.
5. B. Soja, R. Heinkelmann, and H. Schuh. Solar corona electron densities from VLBI and GIM data. In P. Willis and C. Rizos, editors, *Proceedings of the IAG Scientific Assembly 2014*, accepted, 2014.
6. H. Schuh and D. Behrend. VLBI: A fascinating technique for geodesy and astrometry. *J. Geodyn.*, 61:68–80, 2012.
7. M. Pätzold, M. Hahn, S. Tellmann, B. Häusler, M. K. Bird, G. L. Tyler, S. W. Asmar, and B. T. Tsurutani. Coronal Density Structures and CMEs: Superior Solar Conjunctions of Mars Express, Venus Express, and Rosetta: 2004, 2006, and 2008. *Solar Physics*, 279(1):127–152, 2012.
8. M. K. Bird, H. Volland, M. Pätzold, P. Edenhofer, S. W. Asmar, and J. P. Brenkle. The coronal electron density distribution determined from dual-frequency ranging measurements during the 1991 solar conjunction of the ULYSSES spacecraft. *Astrophysical Journal*, 426(1):373–381, 1994.
9. H. Schuh and J. Böhm. Very Long Baseline Interferometry for Geodesy and Astrometry. In G. Xu, editor, *Sciences of Geodesy II: Innovations and Future Developments*. Springer Berlin Heidelberg, 2013.
10. A. Whitney. *Precision Geodesy and Astrometry Via Very-long-baseline Interferometry*. PhD thesis, Massachusetts Institute of Technology, 1974.
11. G. E. Brueckner, R. A. Howard, M. J. Koomen, C. M. Korendyke, D. J. Michels, and J. D. Moses. The Large Angle Spectroscopic Coronagraph (LASCO). *Solar Physics*, 162:357–402, 1995.